Journal of Nanoscience and Technology 2(3) (2016) 178–180

ISSN: 2455-0191

Contents List available at JACS Directory

Journal of Nanoscience and Technology

journal homepage: www.jacsdirectory.com/jnst

Low Temperature Synthesis of Tin Oxide Nano Crystallites: Optical and Dielectric Properties

P. Prabakaran, M. Victor Antony Raj, J. Madhavan*

Department of Physics, Loyola College, Chennai – 600 034, Tamil Nadu, India.

ARTICLE DETAILS

Article history:
Received 13 August 2016
Accepted 22 August 2016
Available online 09 September 2016

Keywords:
Tin Oxide
Hydrothermal
Hydrazine Hydrate
Dielectric

ABSTRACT

Tin oxide nanoparticles were successfully synthesized through hydrothermal method at low temperature using hydrazine hydrate. The effect of concentration on the morphology and structure of SnO_2 were comprehensively studied using scanning electron microscopy (SEM) and X-Ray diffraction (XRD). The electronic band structure is analyzed with the interaction of UV radiation. The polarization mechanism in accordance with an applied electric field was examined. Important dielectric parameters like dielectric constant, dielectric loss and ac conductivity are discussed.

1. Introduction

Recently one of important research fields is nanoscience which contains emerging technologies with interdisciplinary fields like physics, chemistry, biology, material science, and medicine [1]. For various industrial applications such as photo-catalyst [2], semiconductor [3] and gas sensor [4], metal oxide nanostructures have been extensively explored. Some prominent metal oxides semiconductor nanomaterials, such as ZnO, In_2O_3 and SnO_2, have attracted considerable attention because of their unique properties and potential application in various nanodevices. Among them, tin oxide (SnO_2) is considered to be one of the most promising candidate for gas sensor as well as semiconductor due to their inherent advantages such as a wide band gap (3.6 eV at 300 K), a large exciton binding energy (130 meV) and a high electron mobility (100-200 $cm^2\ V^{-1}S^{-1}$)[5].

More recently, SnO_2 nanocrystalline material has received a growing attention due to its excellent properties arising out of large surface-to-volume ratio quantum confinement effect, etc.[6-8]. SnO_2 nanoparticle has several morphologies like nanorods, nanowire, nonobelts, nanotubes, hollow spheres, measoporous structure. Various techniques have been developed to form nanocrystalline SnO_2 and to improve the property of these nanostructures. The properties of SnO_2 nanostructure can be enhanced by a number of ways like impurity adding (doping) [9]. Coating with surfactants [10] and annealing [11]. The final properties of doped SnO_2 nanoparticles are linked to both compositional and processing method. Tin oxide nanomaterials have been prepared by various methods such as sol-gel, hydrothermal, co-precipitation, elctro-deposition, microwave technique, solvothermal, sonochemical, mechanochemical etc. [12]. The hydrothermal method has been considered as a versatile route for the synthesis of SnO_2 nanostructures with controlled size and shape [13].

In this work, we focus the structural and morphological analysis of SnO_2 nanoparticles prepared by hydrothermal method and the energy band structure is studied by the UV interaction. A detailed dielectric spectroscopy is also exemplified.

2. Experimental Methods

In the preparation of tin oxide or stannic oxide, tin chloride penta hydrate ($SnCl_4.5H_2O$) and ($N_2H_4.H_2O$) hydrazine hydrate were used as precursors. $SnCl_4.5H_2O$ was dissolved in 100 mL of double distilled water, then 1.28 g of $N_2H_4.H_2O$ hydrazine hydrate (0.01 M) was added with stirring then it immediately reacted with $SnCl_4$ in the solution to form a slurry-like white precipitate .Then solution was transferred to autoclave at 160 °C for 24 hours and powder was transferred to the centrifuge tubes in order to carry the centrifuge process, maintained at 4000 rpm. After the centrifuge process the solution was transferred to the crucible for 90 °C at 15 hours in furnace in order to make it dry and get the final products.

3. Results and Discussion

3.1 XRD Analysis

The XRD pattern is shown in Fig. 1. The peaks at 2θ values of 26.0°, 34.2°, 37.9°, 51.8° and 65.4° can be associated with (1 1 0), (1 0 1), (2 1 1) and (3 0 1) respectively. The observed peaks are in well agreement with standard X-ray pattern of SnO_2 and confirmed to have a tetragonal structure [14]. The average crystallite size (D) was estimated using the Scherrer's equation as follows

$$D = \frac{K\lambda}{\beta COS\theta}$$

where D is the crystallite size, λ is the X-ray wavelength, β is the full width at half maximum of the diffraction peak, K is a constant (0.94) and θ is the Bragg diffraction angle of the diffraction peaks. The average particle size is found to be 8 nm.

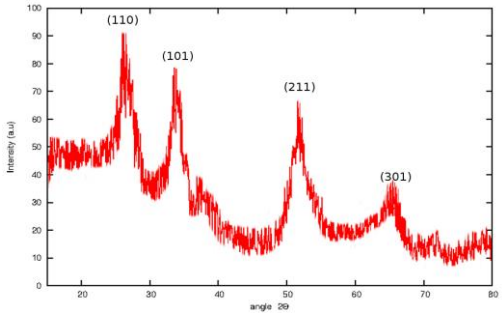

Fig. 1 XRD pattern of the sample SnO_2

*Corresponding Author
Email Address: jmadhavang@yahoo.com (J. Madhavan)

3.2 Morphological Analysis

Scanning Electron Microscopy (SEM) is a vital characterization tool for directly imaging nano materials to obtain quantitative measures of grain size, size distribution, and morphology. Fig. 2 shows the unique morphology of the as-synthesized SnO_2 nano spheres. SEM Micrographs at 1 μm offer better outstanding about passivation of SnO_2 nano particles growth aspect. Images showed the developed shape of the composite and exhibit uniform particles with diameter of 100-120 nm. Further the closest view shows the absence of agglomeration to a large extent in the particles synthesized via hydrothermal method.

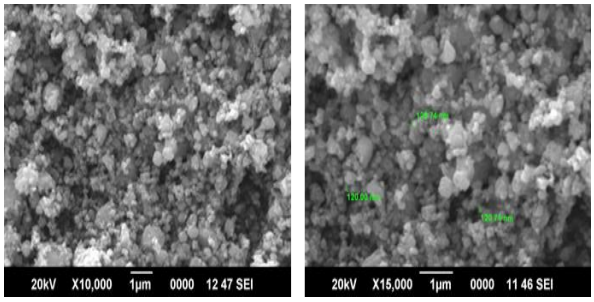

Fig. 2 SEM Micrographs of as-synthesized SnO_2

3.3. UV Spectrum Analysis

The optical transmittance of SnO_2 nanoparticles synthesized by hydrothermal method is measured using VARIAN CARY 5000 spectrophotometer in the range of 200 to 900 nm and is shown in Fig. 3. The spectrum shows a large transparency window between 400 nm and 800 nm and has a sharp absorption edge at about 295 nm. The cut-off behavior at the blue end of the spectrum is determined by direct electronic transitions from valance band to the conduction band. The absorption edge of SnO_2 nano particles possess a blue shift with compared to its bulk material. By combining the transmission with sample thickness, we were able to calculate absorption co-efficient and thus band gap. The calculated E_g value is 4.2 eV which showed that optical band gap widening occurs due to the reduction in particles' size.

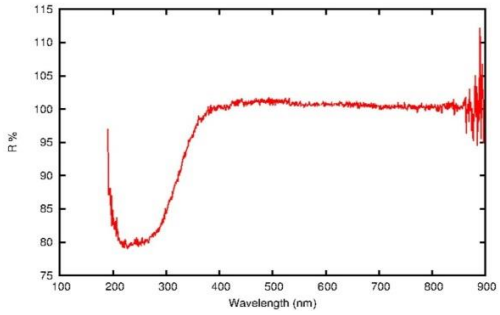

Fig. 3 Reflectance spectra of SnO_2 nanoparticles

3.4. Dielectric Measurements

The prepared SnO_2 nanoparticles got pelletized of area 1.29 cm^2 having silver coating on the opposite faces was introduced between two copper electrodes and then connected to HIOKI LCR impedance analyzer for dielectric measurements. The dielectric constant of the sample is calculated using the relation $\varepsilon_r = Cd/\varepsilon_0 A$; where the SnO_2 pellet acts as a dielectric with the ε_0 absolute permittivity, C is the capacitance, d is the thickness and A is the area. Fig. 4 shows the variation of dielectric constant of SnO_2 nanoparticles in accordance with frequency. From the figure one can easily examine the relative permittivity is higher at lower frequencies and decreases with increase in frequency. The decrement in the value is shown in the frequency window of 50 Hz to 1 kHz and it remains almost constant while we are moving to higher frequencies. The value of dielectric constant is 140 at 50 Hz and it reduces up to 34 at 1 kHz frequency region. At low frequencies, all the four polarizations are active. The orientation effect can sometimes be seen in some materials even up to 10^{10} Hz. Ionic and electronic polarizations always exist below 10^{13} Hz. It is well known that there are two dielectric polarization mechanisms that contribute to the enhanced dielectric behavior of nanomaterials: rotation direction polarization (RDP) process and space charge polarization (SCP) process. We suggest that both RDP and SCP process contribute to the enhancement of dielectric response of the SnO_2. As for the typical n-type semiconductor, there are a large amount of oxygen vacancies acting as shallow donors in SnO_2, resulting in a lot of oxygen vacancies existing in the interfaces of SnO_2 nanoparticles. Positive oxygen vacancies together with negative oxygen ions give a large amount of dipole moments. These dipole moments will rotate in an external electric field, which leads to the rotation direction polarization occurring in the interfaces of n-type SnO_2 nano particles. On the other hand, SCP process can also occur in the sample. Generally, nanostructure materials have about 10^{19} interfaces/cm^3, much more than those of bulk solids.

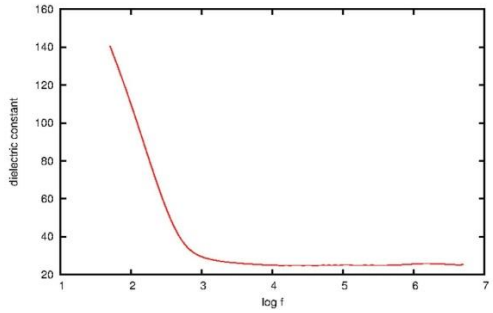

Fig. 4 The variation of dielectric constant with frequency

Negative and positive space in interfaces move towards positive and negative poles of the electric field respectively. As they are trapped by defects, dipole moments will form and SCP process will occur in the sample. Because the volume fraction of the interfaces of nano-size sample is larger than that of bulk materials, SCP is stronger than that in the bulk materials. Thus, ε_r of the SnO_2 nanoparticles is higher than that of bulk. Nevertheless, in the high frequency range, dielectric response of RDP and SCP cannot keep up with the electrical field frequency variation, resulting in the rapid decrease of ε_r in SnO_2 nanoparticles.

Fig. 5 shows the variation of dielectric loss of SnO_2 nanoparticles as a function of frequency. The term, dielectric loss is associated with the energy loss while the electric field passes through the sample. The trend in the variations of both dielectric constant and dielectric loss as a function of frequency is the same. In the lower frequency region, dielectric loss shows larger values due to the loss associated with dipolar movement. Moving to higher frequencies, dipoles cannot align in accordance with electric flux reversals so that less energy loss. The a.c conductivity of SnO_2 is calculated using the relation: $\sigma_{ac} = 2\pi f \varepsilon_0 \varepsilon_r tan\delta$, Where, f is the frequency of applied field, tan δ is loss tangent (ratio of imaginary part of dielectric permittivity to real part of dielectric permittivity) available from dielectric measurement, ε_r is the relative permittivity of the sample and ε_0 is the dielectric permittivity of vacuum (8.854 x 10^{-12} F/m). The alternating current conductivity is directly proportional to frequency and is well examined with Fig. 6.

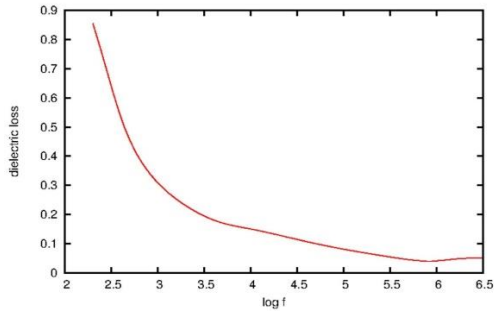

Fig. 5 The variation of dielectric loss with frequency

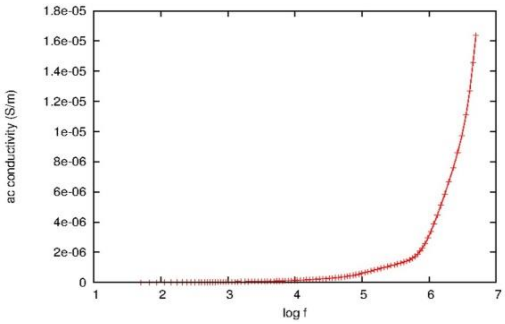

Fig. 6 Variation of ac conductivity with electric field frequency

4. Conclusion

SnO_2 nanoparticles have been successfully synthesized by a simple hydrothermal method using hydrazine hydrate. X-ray spectra indicated that the preparation method was faithful and the crystalline structure was observed to be tetragonal. The surface morphology was investigated by SEM. The dielectric properties of the as-synthesized particles are analyzed. The optical band gap of the SnO_2 was found to be 4.2 eV.

References

[1] G. Madhumitha, S.M. Roopan, Devastated crops: multifunctional efficacy for the production of nanoparticles, J. Nanomat. 13 (2013) 1-12.

[2] H.N. Tien, V.H. Luan, L.T. Hoa, N.T. Khoa, S.H. Hahn, et al, One-pot synthesis of areduced graphene oxide-zinc oxide sphere composite and its use as a visible light photocatalyst, Chem. Engg. J. 229 (2013) 126-133.

[3] G. Thennarasu, A. Sivasamy, S. Kavithaa, Synthesis, characterization and catalytic activity of nano size semiconductor metal oxide in a visible light batch slurry photo reactor, J. Mol. Liq. 179 (2013) 18-26.

[4] D. Wang, X. Chu, M. Gong, Gas-sensing properties of sensors based on single-crystalline SnO_2 nanorods prepared by a simple molten-salt method, Sens. Actuators B Chem. 11 (2006) 183-187.

[5] M. Batzill, U. Diebold, The surface and materials science of tin oxide, Prog. Surf. Sci. 79 (2005) 47-154.

[6] H.C. Chiu, C.S. Yeh, Hydrothermal synthesis of SnO_2 nanoparticles and their gas-sensing of alcohol, J. Phys. Chem. C 111 (2007) 7256-7259.

[7] T.P. Hulser, H. Wiggers, F.E. Kruis, A. Lorke, Nanostructured gas sensors and electrical characterization of deposited SnO_2 nanoparticles in ambient gas atmosphere, Sens. Actuators B 109 (2005) 13-18.

[8] P.P. Sahay, R.K. Mishra, S.N. Pandey, S. Jha, M. Shamsuddin, AC transport properties of nanocrystalline SnO_2 semiconductor, Ceram. Int. 38 (2012) 1281-1286.

[9] A.F. Cabrera, A.M. Mudarra Navarro, C.E. Rodriguez Torres, F.H. Sanchez, Mechanosynthesis of Fe-doped SnO_2 nanoparticles, Phys. B 398 (2007) 215-218.

[10] K. Kamalpreet, A. Mahajan, R.K. Bedi, Effect of cationic/anionic surfactants on evaporation induced self-assembled SnO_2 nanostructured films, J. Appl. Surf. Sci. 257 (2011) 2929-2934.

[11] M.L. Cukrov, T. Tsuzuki, P.G. McCormick, SnO_2 nanoparticles prepared by mechanochemical processing, Script. Mater. 44 (2000) 1787-1790.

[12] S. Gautam, A. Thakur, A. Vij, J. Suk, Ik-Jae Lee, et al, X-ray spectroscopy study of $Zn_x Sn_{1-x} O_2$ nanorods synthesized by hydrothermal technique, Thin Solid Films 546 (2013) 250-254.

[13] H. Hayashi, Y. Hakuta, Hydrothermal synthesis of metal oxide nanoparticles in supercritical water, Mat. 3 (2010) 3794-3817.

[14] E. Ganesh Patil, D. Dnyaneshwar Kajale, B. Vishwas Gaikwad, H. Gotan Jain, Preparation and characterization of SnO_2 nanoparticles by hydrothermal route, Inter. Lett. 2 (2012) 17-21.

Cite this Article as: P. Prabakaran, M. Victor Antony Raj, J. Madhavan, Low temperature synthesis of tin oxide nano crystallites: optical and dielectric properties, J. Nanosci. Tech. 2(3) (2016) 178–180.